Article:
Nicolleau, F. and Yu, G. (2007) Turbulence with combined stratification and rotation: Limitations of Corrsin's hypothesis. Physical Review E, 76. 066302. ISSN: 1550-2376

https://doi.org/10.1103/PhysRevE.76.066302

Published paper
Nicolleau, F. and Yu, G. (2007) *Turbulence with combined stratification and rotation: Limitations of Corrsin's hypothesis,* Physical Review E, Volume 76.

Turbulence with combined stratification and rotation, limitations of Corrsin's hypothesis

F. Nicolleau*
Mechanical Engineering, The University of Sheffield Mapping Street, Sheffield, S1 3JD, United Kingdom

G. Yu
Department of Engineering, Queen Mary, University of London
(Dated: September 24, 2007)

The properties of one-particle and particle-pair diffusion in rotating and stratified turbulence are studied by applying the Rapid Distortion Theory to a Kinematic Simulation of the Boussinesq equation with a Coriolis term. We discuss the simplified Corrsin hypothesis and restrict the validity of its predictions to pure rotation. We emphasize the existence of two τ-regimes driven by very different physics when rotation is present. Particular attention is given to the locality-in-scale hypothesis for two-particle diffusion both in the horizontal and the vertical directions.

PACS numbers: 47.27.Qb 47.27.Eq

I. INTRODUCTION

Rapidly rotating turbulence with or without stratification is to be found in many geophysical or industrial flows.

In this paper the flow field is described by the simplified Boussinesq approximations based on Rapid Distortion Theory (RDT). We use the Kinematic Simulation (KS) discussed in [20] (see references therein). More details of the RDT model on stratified and rotating turbulence can also be found in [2]. This paper addressed the question of the validity of Corrsins simplified hypothesis, which states the equivalence between Eulerian and Lagrangian correlations. Vertical correlations were found to follow this postulate, but not the horizontal ones.

The properties of one-particle and particle-pair diffusion in high Reynolds number and low Froude number stably stratified non decaying turbulence were presented in detail in [17].

The properties of one-particle and particle-pair diffusion in rotating and stratified turbulence were studied in [20].

KS are a very good tool for understanding the role of the linear terms in the Boussinesq equation and our results show that these terms can explain many features concerning one- and two-particle diffusion. Our approach is to understand fully their role before moving on to more complex models.

In Kinematic Simulation (KS), in order to derive the Lagrangian trajectories one has to integrate an "a priori" Eulerian velocity field:

$$\frac{d\mathbf{x}}{dt} = \mathbf{u}(\mathbf{x}, t) \tag{1}$$

knowing the initial conditions for the fluid element (alias particle in this paper) $\mathbf{x}_0$ and $\mathbf{u}(\mathbf{x}_0, 0)$. After its release the particle will experience the action of all scales, and KS must therefore retain information about all scales not only large ones. Hence in KS the velocity field $\mathbf{u}(\mathbf{x}, t)$ is modelled with the same accuracy from the largest down to the smallest scale.

KS were first developed for homogeneous isotropic turbulence where incompressibility and an energy power law spectrum were prescribed [e.g. 3, 5, 6, and references therein]. It appears from [4, 13, 15] that for many Lagrangian properties no particular time-dependence needs to be introduced and a 'frozen' 3-D Eulerian velocity field can generate many Lagrangian properties of the turbulence. The three-dimensionality of streamlines ensures all the necessary time-decorrelations to obtain ballistic régime, random walk régime and Richardson régime for particle pairs initially separated by η the Kolmogorov length scale [19].

For stably stratified flows an analysis of the Lagrangian velocity time-correlation [2, 9, 17] shows that its time-dependence is far more complex than for homogeneous isotropic turbulence and is crucial for the prediction of particle diffusion along the axis of stratification.

Comparisons of KS results with RDT and DNS results can be found in [2], additional DNS results can also be found in [11].

In this paper, we consider a flow subjected to both stratification and rotation characterised respectively by a Brünt-Väissälä frequency N and a rotation rate $\mathbf{\Omega}$. We investigate one and two-particle diffusion along the vertical axis and in the plane orthogonal to the vertical axis. The rotation $\mathbf{\Omega}$, gravity and mean density gradient are all in the direction of the vertical axis referred to as the third axis throughout this paper: $\mathbf{\Omega} = (0, 0, \Omega)$, $\mathbf{g} = (0, 0, -g)$. The stratification is stable and the turbulence non-decaying.

In § II we introduce the KS model and its notations, we also introduce the locality-in-scale assumption as it is to be discussed in this paper. Results for the combined

*Electronic address: Emailaddress:F.Nicolleau@Sheffield.ac.uk

effect of stratification and rotation are given in § III for one-particle statistics and in § IV for particle-pair statistics. Section V summarises this paper's main conclusions.

II. EQUATIONS

A. The Boussinesq assumption

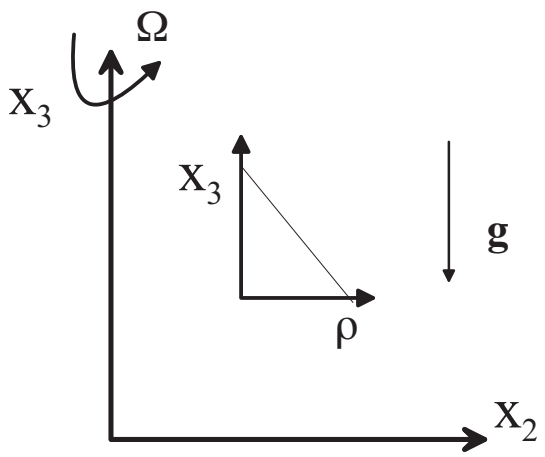

FIG. 1: Stratification and rotation direction.

Our KS is based on the Boussinesq assumption. We consider a stably stratified fluid at static equilibrium, with pressure $p(x_3)$ and density $\rho(x_3)$ varying only in the direction of stratification that is along the vertical axis x_3 (see figure 1). Hence $dp/dx_3 = -\rho g$ where $\mathbf{g} = (0, 0, -g)$ is the gravitational acceleration and we set $\mathbf{x} = (x_1, x_2, x_3)$ in cartesian coordinates. Under Boussinesq approximation the perturbation density ρ' is assumed much smaller that the density ρ so that

$$\frac{D}{Dt}\Theta = -u_3 \frac{1}{\rho}\frac{d\rho}{dx_3} \tag{2}$$

where $\Theta = \frac{\rho'}{\rho}$. The rotation intervenes as a coriolis term $2\mathbf{\Omega} \times \mathbf{u}$ superimposed on the stratified flow dynamics:

$$\frac{D\mathbf{u}}{Dt} = -\frac{1}{\rho}\nabla p' + \Theta\mathbf{g} - 2\mathbf{\Omega} \times \mathbf{u}, \tag{3}$$

with $\mathbf{\Omega}$ the rotation vector. In this paper the study is limited to a rotation in the direction of stratification that is $\mathbf{\Omega} = (0, 0, \Omega)$. As in [17] for the sake of simplicity we omit terms describing molecular diffusion and viscosity. Though there is no theoretical difficulty to incorporate these terms, in practice they make computations rather cumbersome. The perturbation velocity $\mathbf{u}(\mathbf{x}, t)$ is also assumed incompressible:

$$\nabla.\mathbf{u} = 0 \tag{4}$$

B. Linearised Boussinesq equations with rotation

Consider an initial velocity field $\mathbf{u}(\mathbf{x}, 0)$ with spatial fluctuations over a wide range of length-scales, the smallest of these length-scales being η. In the limit where the microscale Froude number and the microscale Rossby number are much smaller than 1, i.e. $Fr_\eta \equiv \frac{u(\eta)}{N\eta} \ll 1$ and $Ro_\eta \equiv \frac{u(\eta)}{\Omega\eta} \ll 1$, (where $u(\eta)$ is the characteristic initial velocity fluctuation at scale η), and in the case where $u(\eta)$ corresponds to the smallest characteristic time-scale in the initial flow, the Eulerian Boussinesq equations (2) and (3) may be approximated by their linear counterparts

$$\frac{\partial}{\partial t}\Theta = -u_3 \frac{1}{\rho}\frac{d\rho}{dx_3} \tag{5}$$

$$\frac{\partial}{\partial t}\mathbf{u} = -\frac{1}{\rho}\nabla p' + \Theta\mathbf{g} - 2\mathbf{\Omega} \times \mathbf{u} \tag{6}$$

We use the Fourier transform $\tilde{\mathbf{u}}(\mathbf{k}, t)$ of $\mathbf{u}(\mathbf{x}, t)$ to solve equations (5) and (6) so that the incompressibility constraint (4) is transformed into $\mathbf{k}.\tilde{\mathbf{u}}(\mathbf{k}, t) = 0$ whilst the pressure field gradient is transformed into a vector parallel to $\mathbf{k}$ in Fourier space. Letting $\mathbf{e_3}$ be the unit vector in the direction of stratification and $\mathbf{e_1}$, $\mathbf{e_2}$ two unit vectors normal to each other and to $\mathbf{e_3}$ (so that $\mathbf{x} = x_1\mathbf{e_1} + x_2\mathbf{e_2} + x_3\mathbf{e_3}$ and $\mathbf{g} = -g\mathbf{e_3}$), the Craya-Herring frame (see figure 2) is given by the unit vectors $\hat{\mathbf{k}} = \frac{\mathbf{k}}{k}$, $\mathbf{c_1} = \frac{\mathbf{e_3}\times\mathbf{k}}{|\mathbf{e_3}\times\mathbf{k}|}$ and $\mathbf{c_2} = \frac{\mathbf{k}\times\mathbf{c_1}}{|\mathbf{k}\times\mathbf{c_1}|}$.

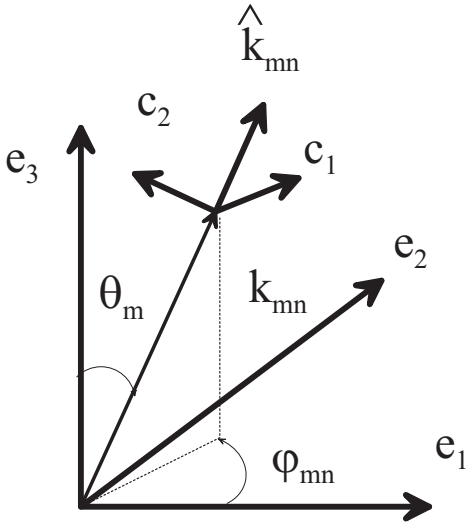

FIG. 2: Craya-Hering frame and Fourier space discretisation.

In the Craya-Herring frame the Fourier transformed velocity field $\tilde{\mathbf{u}}(\mathbf{k}, t)$ lies in the plane defined by $\mathbf{c_1}$ and $\mathbf{c_2}$, i.e.

$$\tilde{\mathbf{u}}(\mathbf{k}, t) = \tilde{v}_1(\mathbf{k}, t)\mathbf{c_1} + \tilde{v}_2(\mathbf{k}, t)\mathbf{c_2}, \tag{7}$$

and is therefore decoupled from the pressure fluctuations which are along $\mathbf{k}$. This decomposition is generic for any

divergence-free velocity field, and related to a classical toroidal-poloidal one in physical space. Where toroidal refers to the component $\tilde{v}_1(\mathbf{k},t)\mathbf{c_1}$ whereas poloidal refers to the component $\tilde{v}_2(\mathbf{k},t)\mathbf{c_2}$. The toroidal mode is purely horizontal, whereas the poloidal mode will yield an horizontal and vertical component.

Incompressible solutions of equations (5) and (6) in Fourier space and in the Craya-Herring frame are [7]:

$$\begin{aligned}\tilde{v}_1(\mathbf{k},t) &= \tfrac{{\sigma_s}^2}{\sigma^2}\tilde{v}_1(\mathbf{k},0) - \tfrac{\sigma_r\, g\sin\theta}{\sigma^2}\tilde{\Theta}(\mathbf{k},0)\\ &+ \left(\tfrac{{\sigma_r}^2}{\sigma^2}\tilde{v}_1(\mathbf{k},0) + \tfrac{\sigma_r\, g\sin\theta}{\sigma^2}\tilde{\Theta}(\mathbf{k},0)\right)\cos\sigma t\\ &+ \tfrac{\sigma_r}{\sigma}\tilde{v}_2(\mathbf{k},0)\sin\sigma t\end{aligned} \quad (8)$$

$$\begin{aligned}\tilde{v}_2(\mathbf{k},t) &= \tilde{v}_2(\mathbf{k},0)\cos\sigma t\\ &- \left(\tfrac{\sigma_r}{\sigma}\tilde{v}_1(\mathbf{k},0) + \tfrac{g\sin\theta}{\sigma}\tilde{\Theta}(\mathbf{k},0)\right)\sin\sigma t\end{aligned} \quad (9)$$

$$\begin{aligned}\tilde{\Theta}(\mathbf{k},t) &= -\tfrac{N}{g}\tfrac{\sigma_r\sigma_s}{\sigma^2}\tilde{v}_1(\mathbf{k},0) + \tfrac{{\sigma_r}^2}{\sigma^2}\tilde{\Theta}(\mathbf{k},0)\\ &+ \tfrac{N}{g}\tfrac{\sigma_s}{\sigma^2}\left(\sigma_r\tilde{v}_1(\mathbf{k},0) + g\sin\theta\ \tilde{\Theta}(\mathbf{k},0)\right)\cos\sigma t\\ &+ \tfrac{N}{g}\tfrac{\sigma_s}{\sigma}\tilde{v}_2(\mathbf{k},0)\sin\sigma t\end{aligned} \quad (10)$$

where $\theta = \theta(\mathbf{k})$ is the angle between $\mathbf{k}$ and $\mathbf{e_3}$, $\sigma_r = 2\Omega\cos\theta$, $\sigma_s = N\sin\theta$, $\sigma = \sqrt{{\sigma_r}^2 + {\sigma_s}^2}$, and the initial conditions are $\tilde{v}_1(\mathbf{k},0)$, $\tilde{v}_2(\mathbf{k},0)$ and $\tilde{\Theta}(\mathbf{k},0)$.

In this paper the study is limited to the case $\tilde{\Theta}(\mathbf{k},0) = 0$ (zero initial potential energy), in which case the equations (8), (9), (10) become

$$\begin{aligned}\tilde{v}_1(\mathbf{k},t) &= \tfrac{{\sigma_s}^2}{\sigma^2}\tilde{v}_1(\mathbf{k},0) + \tfrac{{\sigma_r}^2}{\sigma^2}\tilde{v}_1(\mathbf{k},0)\cos\sigma t\\ &+ \tfrac{\sigma_r}{\sigma}\tilde{v}_2(\mathbf{k},0)\sin\sigma t\end{aligned} \quad (11)$$

$$\tilde{v}_2(\mathbf{k},t) = \tilde{v}_2(\mathbf{k},0)\cos\sigma t - \tfrac{\sigma_r}{\sigma}\tilde{v}_1(\mathbf{k},0)\sin\sigma t \quad (12)$$

$$\begin{aligned}\tilde{\Theta}(\mathbf{k},t) &= -\tfrac{N}{g}\tfrac{\sigma_r\sigma_s}{\sigma^2}\tilde{v}_1(\mathbf{k},0) + \tfrac{N}{g}\tfrac{\sigma_s\sigma_r}{\sigma^2}\tilde{v}_1(\mathbf{k},0)\cos\sigma t\\ &+ \tfrac{N}{g}\tfrac{\sigma_s}{\sigma}\tilde{v}_2(\mathbf{k},0)\sin\sigma t\end{aligned} \quad (13)$$

It is worth here to introduce [2]'s approach (see also [12]): stably stratified turbulence and rotating turbulence can be considered as the superposition of a vortex mode and an internal wave mode. The vortex and internal wave mode are linearly independent, only linked through nonlinear terms in (3). Linear dynamics only affects the wave mode, and consists of periodic exchanges of energy between the wave part of the velocity (identical to the poloidal component only for pure stratification) and the buoyancy field, if stratification is present. In the case of pure rotation, only kinetic energy is concerned, and inertial waves exchange energy between poloidal and toroidal components of the velocity field.

C. KS velocity field

We generalise [17]'s KS velocity field for stratified turbulence. Here, a homogeneous isotropic turbulent field is subjected to rotation with or without stratification. The KS model of turbulent diffusion in rotating or/and stratified non-decaying turbulence consists in solving

$$\frac{d\mathbf{x}}{dt} = \mathbf{u}(\mathbf{x}(t),t) \quad (14)$$

to obtain an ensemble of Lagrangian trajectories $\mathbf{x}(t)$ from the velocity field

$$\begin{aligned}\mathbf{u}(\mathbf{x},t) &= 2\pi\Re\left\{\textstyle\sum_{n=1}^{N_k}\sum_{m=1}^{M_\theta} {k_n}^2\sin\theta_m\Delta k_n\Delta\theta_m e^{i\mathbf{k_{mn}}.\mathbf{x}}\right.\\ &\left.[\tilde{v}_1(\mathbf{k_{mn}},t)\mathbf{c_1}(\mathbf{k_{mn}}) + \tilde{v}_2(\mathbf{k_{mn}},t)\mathbf{c_2}(\mathbf{k_{mn}})]\right\}\end{aligned} \quad (15)$$

where $\Re$ stands for the real part, $\tilde{v}_1(\mathbf{k_{mn}},t)$ obeys equation (11) and $\tilde{v}_2(\mathbf{k_{mn}},t)$ equation (12). $\tilde{v}_1(\mathbf{k_{mn}},0)$, $\tilde{v}_2(\mathbf{k_{mn}},0)$ are specified initial conditions randomly chosen in accordance with an energy spectrum $E(k)$ that has a $-5/3$ large-wavenumber scaling, that is:

$$E(k)\begin{cases}\sim k^{-\frac{5}{3}} & \text{for} \quad k_1 \le k \le k_{N_k} \equiv \frac{2\pi}{\eta}\\ = 0 & \text{otherwise}\end{cases} \quad (16)$$

The spectrum is characterised by the rms value of the velocity fluctuation

$$u'^2 = \frac{2}{3}\int E(k)dk, \quad (17)$$

the integral length-scale

$$L = \frac{3\pi}{4}\frac{\int k^{-1}E(k)dk}{\int E(k)dk}, \quad (18)$$

of the initial isotropic turbulence and the Kolmogorov length scale η. We also introduce t_d the eddy turnover time associated to L and u' as follows

$$t_d = \frac{L}{u'} \quad (19)$$

and τ_η the characteristic time associated to the inner (viscosity simulating) length-scale:

$$\tau_\eta = \left(\frac{\eta}{L}\right)^{\frac{2}{3}} t_d \quad (20)$$

In this paper we choose the values $M_\theta = 20$ and $N_k = 50$ for the cases with both stratification and rotation. For pure rotation it was found that a refined discretisation of the angles θ is needed and we choose $M_\theta = 100$ and $N_k = 30$

Velocity correlations were tested against RDT and DNS results. They have shown satisfactory agreement for most cases $0 \le \frac{2\Omega}{N} \le \infty$ [see 2, for details].

For sake of simplicity we introduce the following notations

$$\begin{cases} \tau & = & t - t_0 \\ \zeta_i(\tau) & = & x_i(t) - x_i(t_0) \\ \Delta_i(\tau) & = & x_i^1(t) - x_i^2(t) \\ \Delta_0 & = & |\mathbf{x}^1(0) - \mathbf{x}^2(0)| \\ \Delta_i^r(\tau) & = & (x_i^1(t) - x_i^1(t_0)) - (x_i^2(t) - x_i^2(t_0)) \\ \delta_i(\tau) & = & \sqrt{< \Delta_i(t)^2 >} \\ \delta_i^r(\tau) & = & \sqrt{< \Delta_i^r(t)^2 >} \end{cases} \quad (21)$$

where t_0 is the time of release of the particle, x_i is the ith component of the particle's position vector $\mathbf{x}$, $\mathbf{x^1}$ refers to the first particle of the particle-pair and $\mathbf{x^2}$ to the second particle of the pair. Subscripts h and v when they are substituted to i indicate respectively horizontal and vertical properties. The strength of the stratification is characterised by the Froude number Fr:

$$Fr = \frac{u'}{LN} \quad (22)$$

and the strength of the rotation by the Rossby number Ro:

$$Ro = \frac{u'}{2L\Omega} \quad (23)$$

When rotation is superimposed on stratification or vice versa, different flow structure interactions result in different behaviours for both one- and two-particle diffusions. A parameter defined as

$$B = \frac{Fr}{Ro} = \frac{2\Omega}{N} \quad (24)$$

is used to classify the turbulence. If $B > 1$ the turbulence is called rotation dominated whereas it is referred to as stratification dominated if $B < 1$.

D. The locality-in-scale hypothesis

The locality-in-scale assumption was introduced in [21] and [1] according to which the pair diffusivity $\frac{d}{dt} < \Delta^2 >$ is mainly sensitive to eddies of size $\delta = \sqrt{< \Delta^2 >}$. For a turbulence spectrum $E(k) \sim k^{-\frac{5}{3}}$ it can easily be shown that this assumption leads to

$$\frac{d}{dt} < \Delta^2 >= \beta u' \eta \left(\frac{L}{\eta}\right)^{-1/3} \left(\frac{\delta}{\eta}\right)^{4/3} \quad (25)$$

and equivalently, to

$$< \Delta^2(\tau) >= G_\Delta \epsilon \tau^3 \quad (26)$$

where we neglect initial separation terms [6, 14]. For an anisotropic flow we can define a coefficient β_h based on the horizontal diffusivity as follows

$$\frac{d}{dt} < \Delta_h^2 >= \beta_h u' \eta \left(\frac{L}{\eta}\right)^{-1/3} \left(\frac{\delta_h}{\eta}\right)^{4/3} \quad (27)$$

In [19] it was shown that the best way to estimate Richardson's locality assumption is to study Richardson's coefficient β defined by equation (25). Though the diffusivity $\frac{d}{dt} < \Delta^2 >$ and the pair rms separation δ are functions of time, time does not appear explicitly in equation (25) which simplifies greatly the study of the effect of the initial condition and enables clear conclusions on the validity of the locality-in-scale assumption. If β is constant then the locality-in-scale assumption is verified, otherwise β will measure the departure from this assumption. We also define χ_i (where $i = 1, 2, 3$ for pair-diffusion in different directions) as the range of $\frac{\delta}{\eta}$ over which the locality assumption is observed. (We discussed in [20] the reasons for extending this interpretation to stratified or rotating turbulence).

III. ONE-PARTICLE DIFFUSION IN STRATIFIED AND ROTATING TURBULENCE

Case	Ω	N	L	u'	$\frac{1}{\eta}$	$\frac{\Delta_0}{\eta}$	B
A	0	500	1	0.35	12.5	1	0
B	100	1000	1	0.35	12.5	1	0.2
C	100	1000	2	0.35	12.5	1	0.2
D	100	1000	1	0.175	12.5	1	0.2
E	100	1000	1	0.35	6.5	1	0.2
F	200	2000	1	0.35	12.5	1	0.2
G	100	1000	1	0.35	12.5	0.02	0.2
H	100	1000	1	0.35	12.5	0.2	0.2
I	100	1000	1	0.35	12.5	5	0.2
J	500	2000	1	0.35	12.5	1	0.5
K	125	500	1	0.35	12.5	1	0.5
L	500	0	1	0.35	12.5	1	∞
M	500	10	1	0.35	12.5	1	100
N	500	100	1	0.35	12.5	1	10
O	2500	500	1	0.35	12.5	1	10
P	500	500	1	0.35	12.5	1	2
Q	500	500	2	0.35	12.5	1	2
R	500	500	1	0.175	12.5	1	2
S	500	500	1	0.35	6.5	1	2
T	1000	1000	1	0.35	12.5	1	2
U	500	500	1	0.35	12.5	0.2	2
V	500	500	1	0.35	12.5	5	2

TABLE I: Different cases studied for particle diffusion in stratified and rotating turbulence.

For different values of B, the results of one-particle diffusion are compared to those obtained in purely stratified turbulence and purely rotating turbulence. The discussion is carried out in terms of $B < 1$ and $B > 1$. In each case, turbulence parameters u', L, η and N or Ω (as long as B is kept constant) are varied. The different cases are reported in table I. The one-particle horizontal and vertical diffusions are investigated separately. Scalings for the one-particle diffusion in both rotation-dominated turbulence and stratification-dominated turbulence are

proposed.

$$< \zeta_i^2(t) >= \int_{t'}^{t} ds' \int_{t'}^{t} < \dot{x}_i(s)\dot{x}_i(s') > ds$$

One popular simplifying hypothesis that has been used for computing particle diffusion is the simplified Corrsin hypothesis which consists in replacing the Lagrangian correlation $< \dot{x}_i(s)\dot{x}_i(s') >$ by its Eulerian counterpart. Furthermore, one can use the linear formula as an estimation for the Eulerian velocities this is the RDT/SCH method introduced in [2].

A. One-particle horizontal diffusion in stratified and rotating turbulence

For pure rotation the formula for horizontal dispersion is given in [2](eq 4.12):

$$< \zeta_h^2(t) >= \frac{\frac{3}{2}u'^2}{8\Omega^2}\left[4\mathrm{Si}(2\Omega t)\Omega t + 2\cos 2\Omega t - \frac{\sin 2\Omega t}{\Omega t}\right] \tag{28}$$

where $\mathrm{Si}(s) = \int_0^s u^{-1}\sin u du$. This equation derived from the simplified Corrsin hypothesis explains the two asymptotic behaviours observed for one-particle horizontal diffusion for pure rotation: The ballistic régime when $\Omega t \to 0$ and the τ-régime when $\Omega\tau \to \infty$. A similar equation can be derived for pure stratification from [2](equation 4.7 with $\sigma_r = 0$):

$$\begin{array}{l} < u_1(t)u_1(t') + u_2(t)u_2(t') >= \frac{3}{2}u'^2 \\ \int_0^1 \left\{1 + \cos^2\theta\cos(Nt\sin\theta)\cos(Nt'\sin\theta)\right\} d\cos\theta \end{array} \tag{29}$$

that is

$$< \zeta_h^2(t) >= \frac{3}{2}u'^2\left\{t^2 + \int_0^1 \left(\cos^2\theta\frac{\sin^2(Nt\sin\theta)}{N^2\sin^2\theta}\right) d\cos\theta\right\} \tag{30}$$

It is worth emphasising here that equation (30) does not contain any information of the turbulence or non-linear characteristic time L/u', so that the τ^2-régime that is known to last up to times of the order of L/u' in the case of pure stratification cannot be related to (30). This is why [2] concluded that the simplified Corrsin hypothesis could not be valid in cases without rotation. In the present paper analysing the particle diffusion rather than just the velocity correlations we can further restrict the validity of this hypothesis to pure rotation only. Furthermore, in § III C we discuss whether RDT/SCH is valid after all.

τ-régimes are of very different natures in pure stratification and pure rotation:

i) In pure stratification the τ-régime is the well-known random walk or Brownian motion that appears when the particle has been diffusing for longer than the turbulence characteristic time, it is independent of N and always appears at a time that scales with L/u'.

ii) In pure rotation the τ-régime is not non-linear or random walk by nature, it is independent of the turbulence characteristic time and appears when the particle has been diffusing for longer than $1/\Omega$ as predicted by (28). To avoid confusion we will refer to this régime as the rotation-τ-régime.

Having that picture in mind it is then easier to understand the main pattern of one-particle horizontal diffusion in a turbulent stratified and rotating flow as illustrated in figure 3.

The ballistic régime yielding a τ^2-law is a common feature in particle diffusion at very small times. It results from the first term of a Taylor expansion of the diffusion as discussed for instance in [18] for stratified turbulence.

In this régime:

$$< (\zeta_h^r)^2 >= (u_h)^2\tau^2 \tag{31}$$

where u_h is a velocity scale function of turbulence parameters. This common ballistic régime will end when the ballistic régime for either the stratification or the rotation is ended that is when

$$\tau > \min\left(\frac{L}{u'}, \frac{1}{\Omega}\right) \tag{32}$$

In the present paper for the KS (and RDT) to be valid we need both $\frac{1}{\Omega}$ and $\frac{1}{N} \ll \frac{L}{u'}$, so that the ballistic régime for the rotation component will always end before the ballistic régime for the stratification component. It is then safe to assume that there will always be a ballistic τ^2-régime up to $1/\Omega$ and a random walk after L/u'. That is after a characteristic time ignored by the Simplified Corrsin Hypothesis (SCH), therefore this hypothesis is not valid whenever $N > 0$.

We need now to discuss what happens when $\frac{1}{\Omega} < \tau < \frac{L}{u'}$.

In figure 4 the horizontal diffusion results are plotted in terms of $< \zeta_h^2 > /L^2$ as a function of τ/t_d, with $B = 0.2$ in all cases. The curves collapse together, and $< \zeta_h^2 > /L^2$ is therefore a universal function of τ/t_d, which reveals that in this stratification-dominated turbulence, the one-particle horizontal diffusion behaves in the same way as in purely stratified turbulence.

This is confirmed in figure 5, when rotation is superimposed on stratification, but $B < 1$ (i.e. $\Omega = 0$ and 125), the one-particle horizontal diffusion barely changes its pattern from the one in purely stratified turbulence. The effect of the superimposed rotation is therefore negligible, although the tendency to have a transition $\tau-$régime between two τ^2-régimes can be already observed when B is close to 1.

As Ω increases and $B > 1$, the diffusion in the early ballistic τ^2-régime is not affected but this régime is shortened, it ends with the rotation ballistic régime which length was shown to scale with $1/\Omega$. This ballistic régime is followed by a τ-régime the length of which increases with B. This τ-régime is the rotation-τ-régime, it is not a random walk régime and in this régime the particle

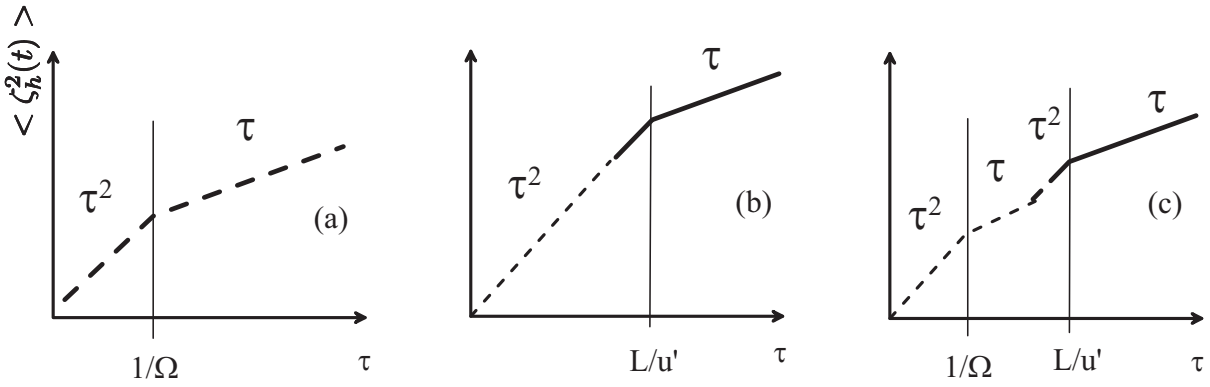

FIG. 3: Schematic scenario of superposition of rotation and stratification diffusion patterns. Dash lines show what can be predicted by the simplified Corrsin hypothesis. (a) pure rotation, (b) pure stratification, (c) rotation and stratification.

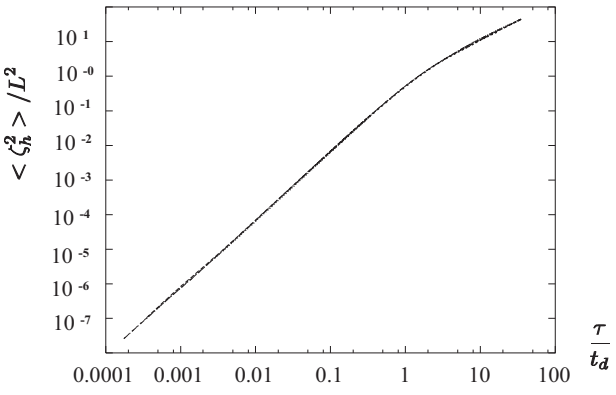

FIG. 4: Non-dimensional one-particle mean square horizontal displacement $< \zeta_h^2 > /L^2$ as a function of τ/t_d in stratification dominant turbulence with $B = 0.2$ for cases B, C, D, E and F in table I.

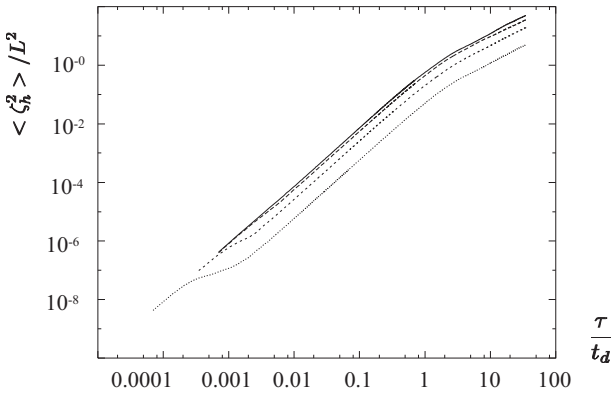

FIG. 5: Effects of rotation on stratification with $N = 500$. Non-dimensional one-particle mean square horizontal displacement $< \zeta_h^2 > /L^2$ is plotted as a function of τ/t_d for cases A, K, P and O in table I, from top to bottom $\Omega = 0$, 125, 500 and 2500.

has not forgotten its initial position. So that for longer times ($\sim 1/N$) when stratification waves develop, a pure stratification pattern - i. e. τ^2 up to L/u' and then a random walk - is superimposed onto the rotation pattern yielding that typical feature of a τ-régime in between two τ^2-régimes as sketched in figure 3.

Figure 5 also shows that the superimposed rotation has no effect on the starting time of the random walk τ-régime.

In rotation-dominated turbulence, $B = 2$, the results of the horizontal diffusion are summarized in figure 6 with two different normalisations and in figure 7 for larger values of B. It is worth noting here that the two τ^2-régimes, with a transition τ-régime were also observed in DNS. [11] found the same results for the one-particle horizontal diffusion in rotating dominant turbulence (i.e. $B > 1$) though they did not specify whether the transition régime was a τ-régime. When examining their figures, one can easily find that this τ-régime is the asymptotic line of the transition range. Although in figure 6 with $B = 2$ this feature is not very evident, it becomes more noticeable when B is increased as shown in figure 7.

This explains the different patterns for $B < 1$ and $B > 1$. By definition when $B < 1$ the stratification is dominant and the mechanisms leading to the rotation structure cannot prevail so that the rotation-τ-régime and the second τ^2-régime are inhibited. Whereas when $B > 1$ the rotation is predominant and the rotation-τ-régime can develop. Figure 7 shows that the onset of this régime driven by rotation is not affected by N; and figure 6-a shows that it scales with $\frac{1}{\Omega}$.

With the normalization adopted in figure 6-a, all the curves collapse together in the two τ^2-régimes and the transition τ-régime, therefore the non-dimensional horizontal diffusion $< \zeta_h^2 > \Omega^2/u'^2$ in these régimes is a universal function of B and $\frac{\Omega\tau}{\pi}$ when $\tau \ll \frac{L}{u'}$. Whereas the non-dimensional horizontal diffusion $< \zeta_h^2 > /L^2$ is found to be a universal function of B τ/t_d in the final random walk τ-régime and the later τ^2-régime as shown in figure 6-b. By the way, the fact that $< \zeta_h^2 > \Omega^2/u'^2$ is a function of $\frac{\Omega\tau}{\pi}$ and that also $< \zeta_h^2 > /L^2$ is a function

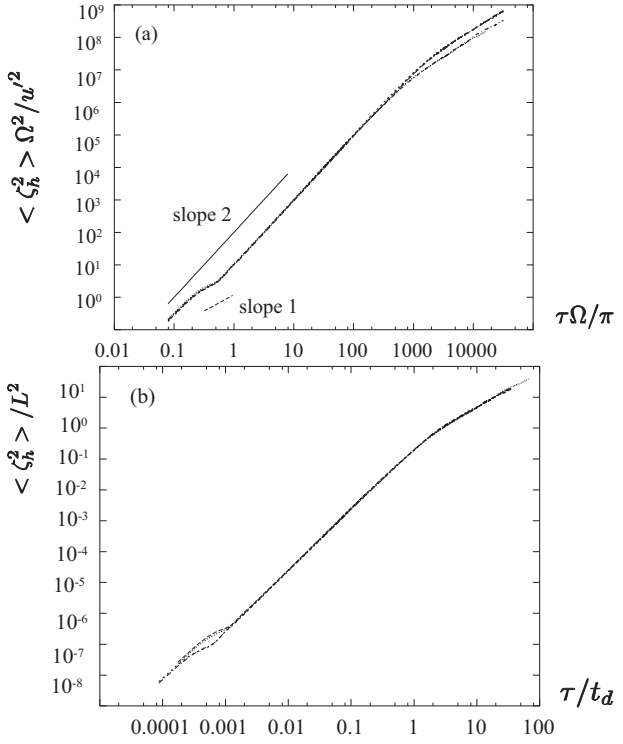

FIG. 6: One-particle mean square horizontal displacement in rotation dominant turbulence with $B = 2$ for cases P, Q, R, S and T in table I. a) $< \zeta_h^2 > \Omega^2/u'^2$ as a function of $\tau\Omega/\pi$. b) $< \zeta_h^2 > /L^2$ as a function of τ/t_d.

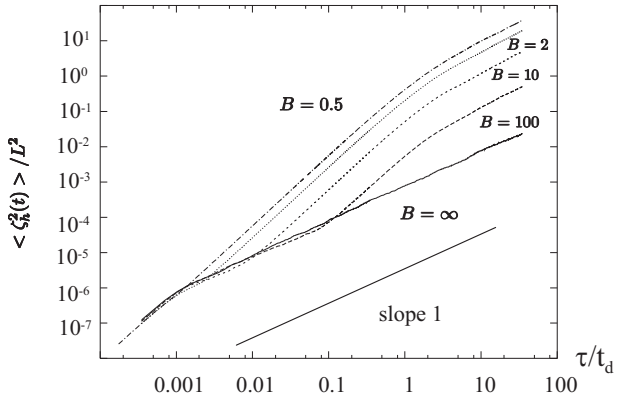

FIG. 7: Effects of stratification on rotation with $\Omega = 500$. Non-dimensional one-particle mean square horizontal displacement $< \zeta_h^2 > /L^2$ is plotted as a function of τ/t_d for cases J, P, N, M and L in table I, from top to bottom $N = 2000$, 500, 100, 10, and 0.

of τ/t_d in this later τ^2-régime, implies $< \zeta_h^2 > \sim (u'\tau)^2$ as already mentioned above.

The main results of having rotation superimposed on stratified turbulence can be summarised as follows:

(1) The time when the random walk régime starts is only a function of L/u' regardless of the value of N or Ω.

(2) As N increases (or B decreases), the transition τ-régime is shortened until finally it disappears when $B < 1$.

(3) The diffusion after the ballistic τ^2-régime increases when B decreases.

(4) No effect of the superimposed stratification on the diffusion in the ballistic τ^2-régime is observed, and this régime finishes at a time related to Ω only.

B. One-particle vertical diffusion in stratified and rotating turbulence

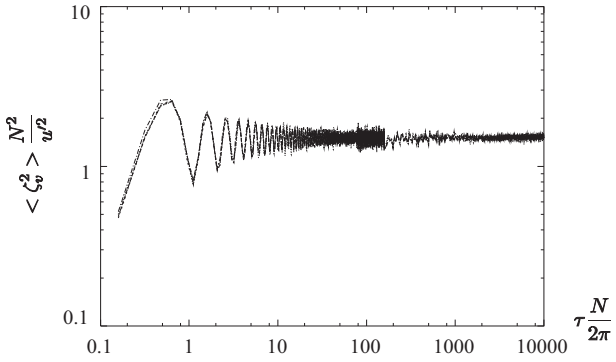

FIG. 8: Non-dimensional one-particle mean square vertical displacement $< \zeta_3^2 > N^2/u'^2$ as a function of $\tau N/2\pi$ in stratification dominant turbulence with $B = 0.2$ for (from top to bottom) cases B, C, D, E and F in table I.

From figure 8 where B equals 0.2, one can see that the non-dimensional vertical diffusion $< \zeta_3^2 > N^2/u'^2$ is a universal function of $\frac{N}{2\pi}\tau$, which shows that the one-particle vertical diffusion in this turbulence also behaves as in purely stratified turbulence. The diffusion pattern does not change very much, the difference is hardly discernable apart from the first loop of the oscillations where the diffusion sometimes shows higher or lower values than the case without rotation.

The superimposed rotation makes a distinctive difference only when the turbulence becomes rotation-dominated, $B > 1$. Figure 9 shows that as Ω increases, the amplitude of the plateau is reduced, moreover, the starting time of the plateau is moved forwards. It is also observed that rotation has no significant influence on the diffusion in the ballistic τ^2-régime except that the régime is shortened as Ω increases.

The results for the vertical diffusion when $B = 2$ are shown in figure 10. The curves plotted the way they are in this figure show a good collapse in this rotation-dominated turbulence case. Minor differences appear at the early stage of oscillations which only weakly affect

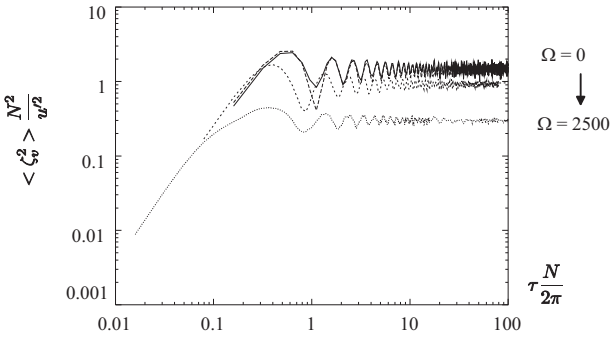

FIG. 9: Effects of rotation on stratification with $N = 500$. Non-dimensional one-particle mean square vertical displacement $< \zeta_3^2 > N^2/u'^2$ is plotted as a function of $\tau N/2\pi$ for the same cases as in figure 5, from top to bottom $\Omega = 0$, 125, 500 and 2500.

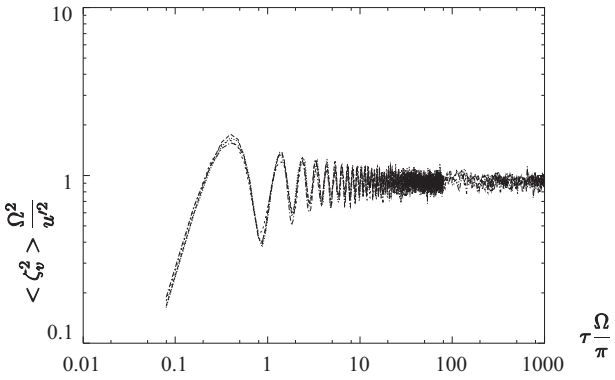

FIG. 10: Non-dimensional one-particle mean square vertical displacement $< \zeta_3^2 > \Omega^2/u'^2$ as a function of $\tau\Omega/\pi$ in rotation dominant turbulence with $B = 2$ for (from top to bottom) cases P, Q, R, S and T in table I.

the normalization around the crests of the first few oscillation periods. Thus the non-dimensional vertical diffusion $< \zeta_3^2 > \Omega^2/u'^2$ is a universal function of $\frac{\Omega\tau}{\pi}$ and B in rotation-dominated turbulence.

Furthermore figure 11 shows that the Coriolis term does not affect the existence of a vertical diffusion capping, though it affects the value of the plateau. This is expected as the analysis conducted in [8, 17] in terms of potential energy is still valid (Coriolis force has no work), thus implying a plateau for vertical diffusion which must scale as

$$< \zeta_3^2 > \simeq f(B)\frac{u'^2}{N^2} \tag{33}$$

Even with a relatively weak stratification, that is $B = 100$, for large times the diffusion pattern has been changed into a pure stratification pattern with a capping of the diffusion in the vertical direction. However, at smaller times it does not faithfully behave as in pure stratification. Instead, it contains an additional transition τ-régime between the ballistic τ^2-régime and the final plateau.

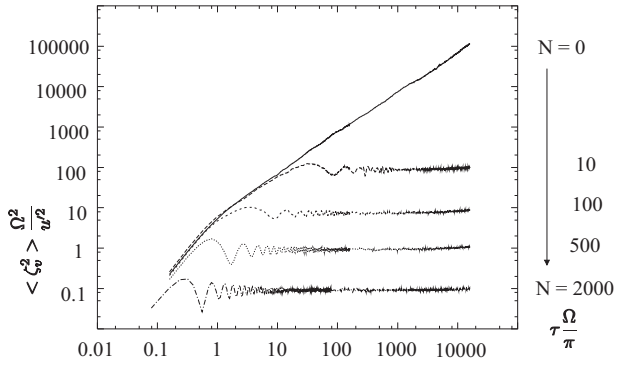

FIG. 11: Effects of stratification on rotation with $\Omega = 500$. Non-dimensional one-particle mean square vertical displacement $< \zeta_3^2 > \Omega^2/u'^2$ is plotted as a function of $\tau\Omega/\pi$ for the same cases as in figure 7, from bottom to top $N = 2000$, 500, 100, 10, and 0.

The beginning of the plateau is governed by the stratification and scales with $\frac{1}{N}$, whereas the transition τ-régime as already mentioned for the horizontal diffusion is an effect of the rotation and its beginning scales with $\frac{1}{\Omega}$ provided that both effects can co-exist that is $\frac{1}{\Omega} < \frac{1}{N}$ or $B > 1$. As N increases, the rotation-τ-régime decreases until it completely disappears when $B < 1$, and the diffusion then follows a pure stratification pattern. Meanwhile, the amplitude of the plateau is decreased as N increases.

It is important to point out here the reason why turbulent parameter values such as $\Omega = 500$, $L = 1$ and $u' = 0.35$ (that is $Ro = 0.00035$) have been chosen in this study. In rotating turbulence with weak stratification, e.g. $B = Fr/Ro = 100$, the diffusion in the vertical direction behaves as in pure stratification. Only with very small values of the Rossby number can one have small enough Froude numbers to make the RDT on which our KS model is based valid.

Figure 12 describes the effect of rotation on the vertical diffusion.

- In any case as already mentioned for $N\tau \gg 1$ a plateau is observed in accordance with the principle of energy conservation.
- A ballistic régime is observed when both stratification and rotation ballistic régimes co-exist that is up to $\tau = \min(\Omega^{-1}, N^{-1})$.
- When stratification is dominant ($B < 1$), the plateau is reached before the rotation waves can develop so that the rotation has no effect on the vertical diffusion.
- When rotation is dominant ($B > 1$), the rotation-τ-régime develops before stratification waves so that the plateau is lowered and a function of both Ω and N.

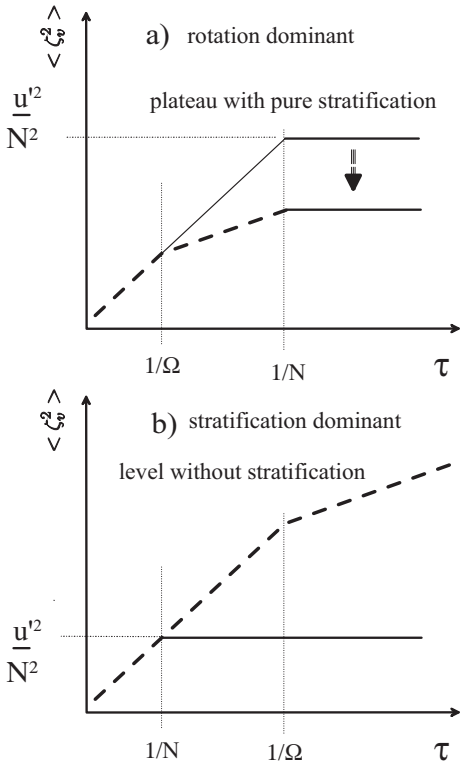

FIG. 12: Schematic scenario of one-particle diffusion when rotation and stratification are superposed. a) for $B > 1$ the rotation pattern settles first and the stratification characteristic plateau appears afterwards. b) for $B < 1$ the stratification plateau appears before the rotation effects start, so that the rotation does not affect the plateau.

C. Is RDT/SCH valid after all?

We have seen that the RDT/SCH is not valid whenever there is some stratification. This is because the Brownian motion that exists in the horizontal direction is not predicted in the RDT/SCH. In the light of this shortcoming it is worth looking back at what was meant here earlier or in [2, 12] when it was said that SCH is valid for pure rotation. The criteria was the comparison with Lagrangian DNS results: SCH is valid in that sense that it predicts the right Lagrangian results.

But superimposing rotation and stratification had made it clear that there are two t-régimes corresponding to two different physics: one due to the wave dynamics (at small time), one corresponding to an actual Brownian motion due to velocity decorrelation (at large time). SCH has only one of the two physics, so it is not in that sense valid because one would expect in a turbulent régime velocity decorrelation to occur eventually, and an actual Brownian motion to exist even with pure rotation.

It is just fortunate that in Lagrangian terms it is not possible, in pure rotation, to discriminate between the two mechanisms. The first mechanism (wave dynamics) is not valid after a turn over time and should be replaced by a Brownian mechanism. The two wrongs of the SCH:

- not having any information about the Brownian mechanism
- carrying on the first mechanism after the turbulence turn over time (or decorrelation)

make a right and in Lagrangian terms the SCH prediction is accurate.

The case $B = 1$ is illuminating in that respect as it can show that the Brownian mechanism is always there, even in the vertical direction when there is stratification. Indeed for $B = 1$ there is no phase mixing and results in [12] show that there is an effect of the non-linear terms. In this case, there is a discrepancy between RDT/SCH and DNS or KS. The discrepancy between DNS and RDT/SCH indicates the presence of the velocity decorrelation, which cannot be discriminated from phase mixing in other cases. The comparison with KS also shows that KS does incorporate the velocity decorrelation. (However, in [12] DNS and KS seem to lose their accuracy at $t > L/u'$ as then the vertical diffusion increases whereas according to the energy argument it should be constant for ever.)

D. Role of spatial structures

KS for stratified turbulence as it is generated in this paper (§ II) does not contain any information about spatial structures such as layers or columns that are observed respectively for stratified turbulence and rotating turbulence recent and higher-resolution results of such structures can be found in [12]. So how important are these structures in the prediction of particles' diffusion? First what matters in Lagrangian tracking is Lagrangian correlations not Eulerian's ones. So it is necessary to get accurate Lagrangian velocity correlation. Comparisons with DNS [2, 12] show that the KS without the Eulerian structures predicts accurately the diffusion for one and two particles for stratified, rotating, and stratified and rotating turbulence.

We refer the reader to [12] for a detail analysis of the poor impact of spatial structures on the particle diffusion. Here, we want to emphasise that layered-structures cannot explain the main feature of diffusion in stratified turbulence that is that the vertical diffusion exhibits a plateau when $N\tau > 1$. Indeed the energy argument that $N^2 < \zeta^2(\tau) >$ must be bounded is valid with or without rotation as the Coriolis force does not work. Therefore whatever B finite there exists a plateau irrespective of the Eulerian spatial structures predominantly layer-like or column-like or neither when $B = 1$.

We can conclude that linear time-oscillations that are contained in KS are necessary and sufficient to predict accurately particle's diffusion in stratified and/or rotating turbulence, whereas Eulerian structures such as layers or columns are neither sufficient nor necessary.

IV. TWO-PARTICLE DIFFUSION IN STRATIFIED AND ROTATING TURBULENCE

In this section, two-particle diffusion is investigated when there is stratification and rotation. We do not discuss here as to the capacity of KS to model two-particle diffusion in general. In particular, we do not comment on the effect of having no explicit sweeping mechanism in our model. The validity of our results is supported by previous research e. g. [19], [22] for two-particles and in [10], [16] who compare KS and experimental results of muti-particle diffusion. All these studies support the use of KS when $L/\eta < 10^4$, (in this paper $L/\eta < 100$). As to the reasons for extending an isotropic hypothesis (Richardson's) to the stratified and rotating turbulence we refer the reader to the discussion in [20].

Pair-diffusions have been studied in [20] for the cases of pure rotation and pure stratification, in this paper we study the combined effect of both rotation and stratification. It is hard, without an energy argument to use or DNS results at large Reynolds number to compare with, to estimate the role the 'Eulerian structures' could have on pair diffusion. For vertical diffusion, when there is stratification we are quite confident from our comparison with [11] that the effect is negligible. When it comes to pair diffusion in the horizontal direction (or along any direction for pure rotation), one wants to see a Richardson régime and compare power laws. It is worth noting in this context that there are already arguments as to whether one can find a Richardson régime in an isotropic DNS. So we could conclude from the fact that we do not observe discrepancy between KS and DNS pair-diffusion for the cases in [11] that the Eulerian structures are not important for two particle dispersion at least for the Reynolds numbers achievable in DNS.

Figures 13 and 14 summarize the diffusion results in stratified and rotating turbulence for the two different values of $B = 0.2$ and 2. Each figure shows a particular aspect of the diffusion at a given value of B.

Features shared in the same range of time by purely rotating and purely stratified turbulence are also observed when both are acting on turbulence. In particular, there is an early-time ballistic τ^2-régime:

$$< \Delta_i^r(\tau)^2 >= \delta v_i^2\, \tau^2$$

It can be seen that when $B = 0.2$, the two-particle diffusion in this stratification-dominated turbulence displays no significant difference from that in purely stratified turbulence in both the horizontal plane and the vertical direction.

However, when $B = 2$, the leading effect of the rotation in horizontal diffusion is to generate a transition $\tau-$régime and a later τ^2-régime different from the early-time ballistic τ^2-régime. Nevertheless, the diffusion in the vertical direction behaves as in purely stratified turbulence, i.e. there are two plateaux in the vertical diffusion (not shown here).

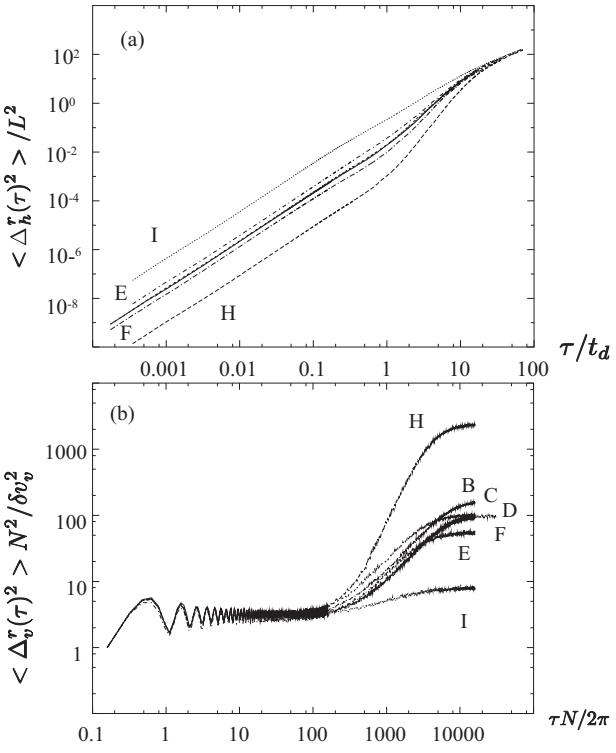

FIG. 13: Non-dimensional pair mean square relative horizontal separation when $B = 0.2$ for cases B, C, D, E, F, H and I in table I. a) $< \Delta_h^r(\tau)^2 > /L^2$ as a function of τ/t_d b) $< \Delta_v^r(\tau)^2 > N^2/\delta v_v^2$ as a function of $\tau N/2\pi$.

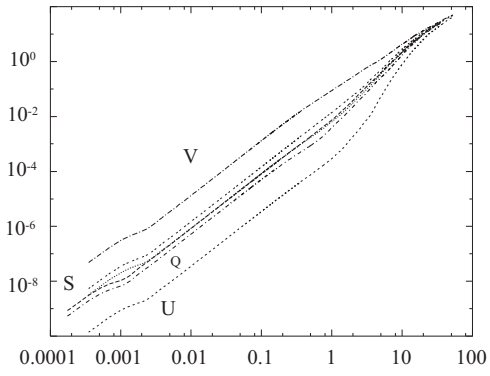

FIG. 14: Non-dimensional two-particle mean square relative horizontal separation with $B = 2$ for cases P to V in table I. $< \Delta_h^r(\tau)^2 > /L^2$ as a function of τ/t_d (middle curves: cases P, R and T)

In the final $\tau-$régime as shown in figures 13 and 14 the non-dimensional mean square horizontal diffusion $< \Delta_h^r(\tau)^2 > /L^2$ is found to be a universal function of τ/t_d for both $B = 0.2$ and $B = 2$.

The two-particle horizontal diffusion at the intermediate times is found to be governed by the locality-in-scale hypothesis. This is investigated in §IV D.

With respect to two-particle diffusion in the vertical direction, as shown in figure 15 the scalings of the first

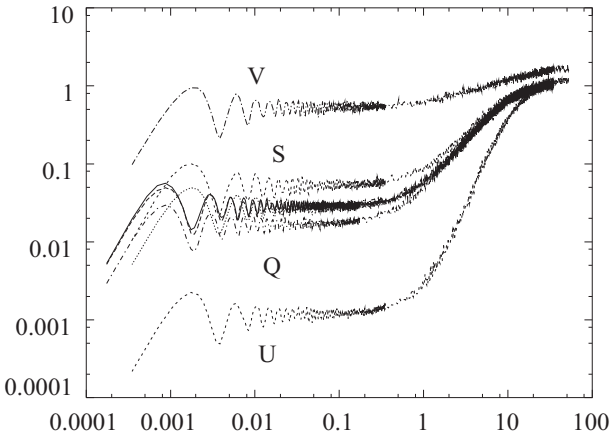

FIG. 15: Non-dimensional two-particle mean square relative vertical separation. $< (\Delta_3^r)^2 > /L^2$ as a function of τ/t_d with $B = 2$ for cases P to V in table I (middle curves: cases P, R and T.

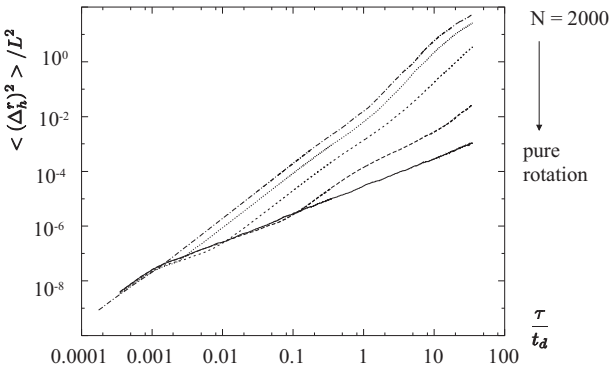

FIG. 16: Effects of stratification on rotation with $\Omega = 500$. Non-dimensional two-particle mean square relative separation in horizontal plane $< (\Delta_h^r)^2 > /L^2$ is plotted as a function of τ/t_d for cases L, M, N, P, and J in table I, from top to bottom $N = 2000$, 500, 100, 10, and 0.

and the second plateau are based on the same parameters as in purely stratified turbulence except that the coefficients in these scalings now depend on the value of B.

A. Effects of superimposed stratification on pair horizontal diffusion in turbulence with constant Ω

Figure 16 presents the effects of superimposed stratification on two-particle horizontal diffusion at a fixed value of Ω. Before the pair enters the intermediate range of time where a Richardson's law could develop, observations similar to the ones made for one-particle diffusion (figure 7) can now be made for the pair horizontal diffusion.

One can see from figure 16 that the superimposed stratification does not affect the diffusion in the ballistic τ^2-régime, but as N increases the diffusion is enhanced

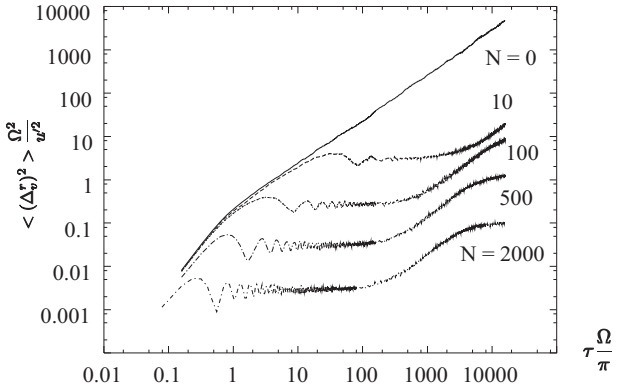

FIG. 17: Effects of stratification on rotation with $\Omega = 500$. Non-dimensional two-particle mean square relative separation in vertical direction $< (\Delta_v^r)^2 > \Omega^2/u'^2$ is plotted as a function of $\tau\Omega/\pi$ for the same cases as in figure 16, from bottom to top $N = 2000$, 500, 100, 10, and 0.

in the subsequent régimes compared with the case without stratification. Furthermore, as the stratification gets stronger the transition $\tau-$régime becomes shorter until it finally disappears or is hardly observed when the stratification becomes dominant.

The final random walk $\tau-$régime for the two-particle diffusion can only be observed when the stratification is strong (see figure 16). As N decreases this régime is delayed and could not be reached for $B \geq 10$. As a result the diffusion at intermediate times is not displayed completely. Since the Rossby number considered here is very small, $Ro = 0.00035$, it would require a much longer simulation time to reach the final random walk régime.

B. Effects of superimposed stratification on pair vertical diffusion in turbulence with constant Ω

In the vertical direction, figure 17 shows that even a very weak stratification can lead to a diffusion pattern dramatically different from the one in purely rotating turbulence. After a certain time the diffusion is capped and a plateau appears, as it would for pure stratified turbulence. If N is large enough a second plateau can also be observed.

The figure also shows that when N is very small, that is $B \gg 1$, the diffusion behaves as in pure rotation for a certain period of time,with a $\tau-$régime followed by the first plateau. When rotation is an overwhelmingly dominant factor of the turbulence, the ballistic τ^2-régime finishes at a time independent of N but function of Ω. Nevertheless, the times when the first plateau starts and stops are determined by N rather than Ω; a smaller N corresponds to a later appearance and a later termination of the first plateau.

As N increases the $\tau-$régime gets shorter until it finally disappears when the stratification becomes dominant, and the diffusion then follows a pure stratification

pattern. Furthermore, an increment of N only slightly reduces the diffusion in the ballistic τ^2-régime but considerably decreases the levels of the two plateaux.

With the parameters chosen here, one can only observe the second plateau in the case of $N = 2000$. Provided that enough computation time is available the second plateau can be obtained for all the cases except $N = 10$ as in this case the Froude number is not small enough to make the KS model valid for such a long time.

C. Effects of superimposed rotation on diffusion in turbulence with constant N

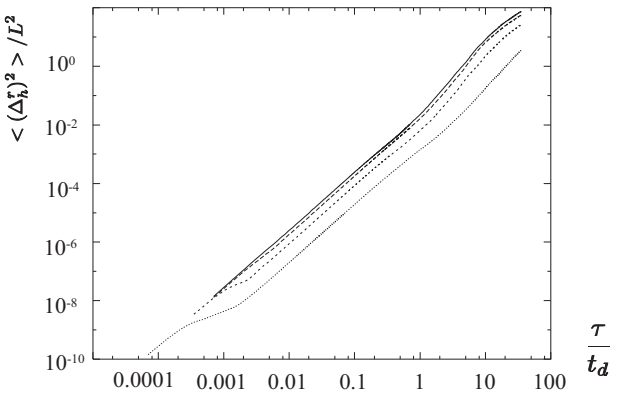

FIG. 18: Effects of rotation on stratification with $N = 500$. Non-dimensional two-particle mean square relative separation in horizontal plane $< (\Delta_h^r)^2 > /L^2$ is plotted as a function of τ/t_d for cases A, K, P and O in table I, from top to bottom $\Omega = 0$, 125, 500 and 2500.

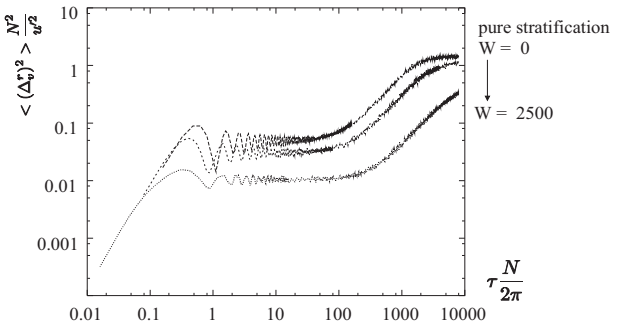

FIG. 19: Effects of rotation on stratification with $N = 500$. Non-dimensional two-particle mean square relative separation in vertical direction $< (\Delta_v^r)^2 > N^2/u'^2$ is plotted as a function of $\tau N/2\pi$ for the same cases as in figure 18, from top to bottom $\Omega = 0$, 125, 500 and 2500.

Figures 18 and 19 illustrate the effects of superimposed rotation on the two-particle diffusion in turbulence with a fixed value of N. In the horizontal diffusion, if the rotation is weak that is $B < 1$, the diffusion is slightly affected. As Ω increases, a more obvious transition $\tau-$régime arises and shifts to an earlier time. In the mean time, the diffusion is reduced, and the final $\tau-$régime is postponed until there is no such régime observed in the case of $\Omega = 2500$. It is also shown that the introduction of rotation has no effect on the diffusion in the ballistic τ^2-régime but shortens it, furthermore, the later τ^2-régime also finishes at a time independent of Ω but a function of L/u'.

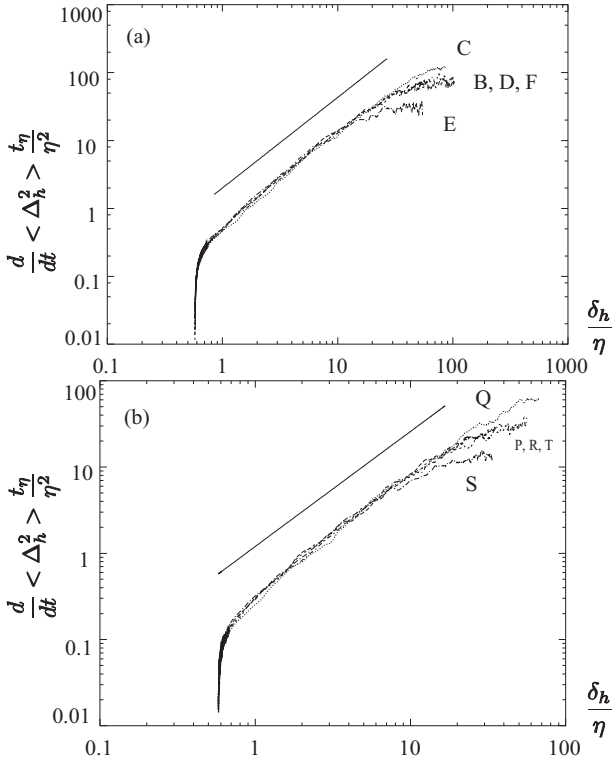

FIG. 20: Non-dimensional two-particle horizontal diffusivity $\frac{d}{dt} < \Delta_h^2 > \frac{t_\eta}{\eta^2}$ as a function of δ_h/η. The solid line represents Richardson's four-third diffusivity law. a: $B = 0.2$ for cases B to F in table I. b: $B = 2$ for cases P to T in table I.

As for the diffusion in the vertical direction, it is shown that a weak rotation can not alter the diffusion very much until it becomes dominant over stratification, i.e. $B > 1$. As Ω increases, the diffusion in the ballistic τ^2-régime is not affected significantly, by contrast the levels of the two plateaux are further decreased. Meanwhile, the first plateau starts earlier but finishes at a later time and as a consequence the second plateau's appearance is postponed.

D. Investigation of the locality-in-scale hypothesis

As shown in figures 20 and 21, the two-particle horizontal diffusion in the intermediate range of times is found to be governed by Richardson's four-third diffusivity law. For a given value of B, Richardson's coefficient β_h is an increasing function of Δ_0/η, and the law is valid in a range determined by L/η and Δ_0/η.

Here as well the identical effects of stratification and

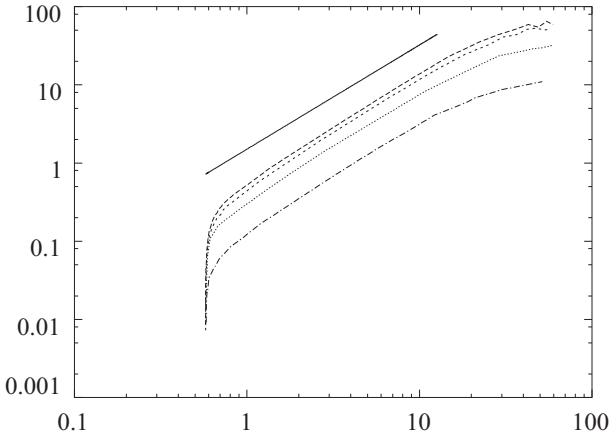

FIG. 21: Effects of B on two-particle diffusivity in rotating and stratified turbulence. Non-dimensional horizontal diffusivity $\frac{d}{dt} < \Delta_h^2 > \frac{t_\eta}{\eta^2}$ is plotted as a function of δ/η. From top second to bottom $B = 0$, 0.5, 2 and 10. Other parameters are $L = 1$, $1/\eta = 12.5$, $u' = 0.35$ and $\Delta_0/\eta = 1$. Solid line has a slope of 4/3 representing Richardson's four-thirds diffusivity law.

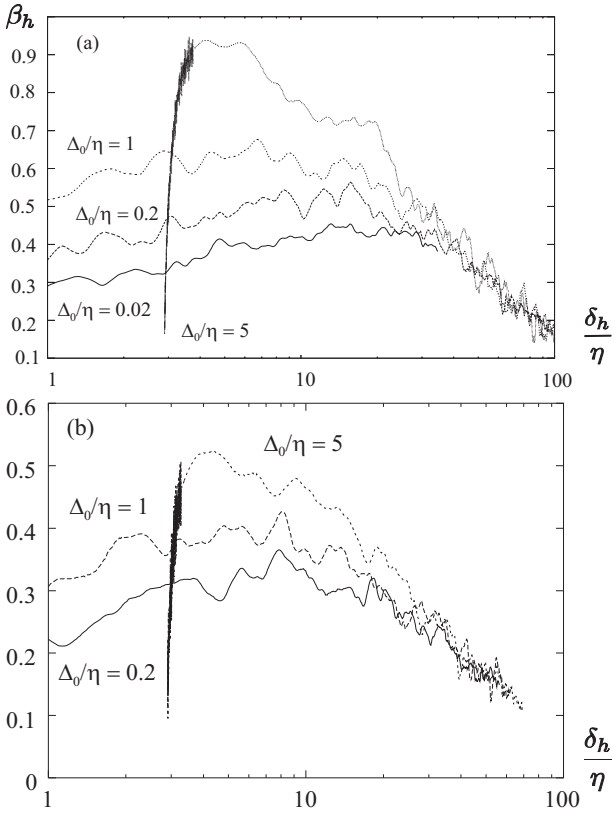

FIG. 22: β_h as a function of δ_h; a) $B = 0.2$ for cases B, G, H and I in table I; b) $B = 2$ for cases P, U and V in table I.

rotation on turbulence pair diffusion will be retrieved when both are present at the same time. In particular, whatever the value of B, rotation and stratification's overall effect is to decrease the diffusion and improve the locality assumption.

More can be deduced on the locality-in-scale hypothesis and Richardson's diffusivity law in rotating and stratified turbulence. It can be seen that in figure 20, at a fixed value of B and Δ_0/η all the curves collapse with the line representing Richardson's four-third diffusivity law regardless of the turbulent parameters L, u', η, N or Ω. This means that at a given B and Δ_0/η, Richardson's coefficient β_h does not depend on the turbulent parameters, whereas the range χ_h depends on L/η.

Figure 22 shows the effect of the initial separation on β_h for $B = 0.2$ and 2. Whether B equals 2 or 0.2, for a given value of Δ_0/η, the variation of β_h in Richardson's four-third range is negligible, it can hence be treated as a δ-independent coefficient that increases with Δ_0, the locality-in-scale hypothesis then applies to any initial separation. It can also be seen that χ_h decreases with Δ_0/η when $\Delta_0/\eta > 1$.

Comparing figure 20-a and -b, that is $B = 0.2$ and 2, one can see that the value of β_h differs, which implies that at a constant Δ_0/η, β_h is only a function of B.

As shown in figure 21, as B increases the value of β_h is reduced compared with the case without rotation. However B has no significant effect on χ_h.

So to summarize Richardson's coefficient β_h is Δ_0-dependent. Its value increases with Δ_0/η but decreases with B. Whilst χ_h is independent of B and determined by L/η and Δ_0/η, it increases with L/η and decreases with Δ_0/η when $\Delta_0/\eta > 1$.

V. CONCLUSION

In the paper we use KS coupled with Rapid Distortion Theory to model one and two-particle diffusion in turbulence with stratification and rotation. We show that the simplified Corrsin hypothesis introduced in [2] has to be restricted to pure rotation only.

One-particle and two-particle diffusion is investigated in horizontal and vertical direction. For one-particle horizontal dispersion we observe four regimes:

- the ballistic regime when $\tau < 1/\Omega$
- a intermediary τ-regime which is not the random walk
- followed by a τ^2-regime up to $\tau \simeq L/u'$
- and finally the random walk τ-regime when $\tau > L/u'$

For one-particle vertical diffusion the effect of rotation is to lower the diffusion's plateau. A plateau is always observed as soon as there is stratification in accordance with the principle of energy conservation. We conclude that the Eulerian spatial structure that exists in real flows but not in KS plays a minor role in the vertical capping observed in stratified flows.

When considering two-particle diffusion, adding rotation to stratification has the same effect in the ballistic regime as the one observed for one-particle. I.e. it introduces an intermediary τ-regime which delays all the subsequent regimes.

We analyse the locality-in-scale hypothesis in the intermediary range of times and adopt [19]'s approach to study β_h as a function of $\frac{\delta_h}{\eta}$. We conclude that β_h does not depend on the turbulence's parameters but on B. Whereas, χ_h the range other which β_h is close to a constant is independent of B and a function of the turbulence's parameters.

Acknowledgments

FN and GY acknowledge EPSRC sponsorship N° GR/N22601, EPSRC UK Turbulence Consortium and GR/R64957/01

[1] Batchelor, G. K. 1952 The effect of homogeneous turbulence on material lines and surfaces. *Proc. Roy. Soc. London A* **213**, 349.

[2] Cambon, C., Godeferd, F. S., Nicolleau, F. & Vassilicos, J. C. 2004 Turbulent Diffusion In Rapidly Rotating Turbulence With or Without Stable Stratification. *J. Fluid Mech.* **499**, 231–255.

[3] Elliott, F. W. & Majda, A. J. 1996 Pair dispersion over an intertial range spanning many decades. *Phys. Fluids* **8** (4), 1052–1060.

[4] Flohr, P. & Vassilicos, J. C. 2000 Scalar subgrid model with flow structure for large-eddy simulations of scalar variances. *J. Fluid Mech.* **407**, 315–349.

[5] Fung, J. C. H., Hunt, J. C. R., Malik, N. A. & Perkins, R. J. 1992 Kinematic Simulation of homogeneous turbulence by unsteady random Fourier modes. *J. Fluid Mech.* **236**, 281–317.

[6] Fung, J. C. H. & Vassilicos, J. C. 1998 Two-particle dispersion in turbulentlike flows. *Phys. Rev. E* **57** (2), 1677–1690.

[7] Godeferd, F. S. & Cambon, C. 1994 Detailed investigation of energy transfers in homogeneous stratified turbulence. *Phys. Fluids* **6**, 2084–2100.

[8] Hanazaki, H. & Hunt, J. C. R. 1996 Linear processes in unsteady stably stratified turbulence. *J. Fluid Mech.* **318**, 303–337.

[9] Kaneda, Y. & Ishida, T. 2000 Suppression of vertical diffusion in strongly stratified turbulence. *J. Fluid Mech.* **402**, 311–327.

[10] Khan, M. A. I., Pumir, A. and Vassilicos J. C. 2003 Kinematic Simulation of multipoint turbulent diffusion *Phys. Rev. E* **68**, 026313.

[11] Kimura, Y. & Herring, J. R. 1999 Particle dispersion in rotating stratified turbulence. *Proceedings of FEDSM99* **FEDSM99-7753**.

[12] Liechtenstein, L., Cambon, C. & Godeferd, F. 2005 Nonlinear formation of structures in rotating stratified turbulence. *Journal of Turbulence* **6** (24), 1–18.

[13] Malik, N. A. & Vassilicos, J. C. 1996 Eulerian and Lagrangian Scaling Properties of Randomly Advected Vortex tubes. *J. Fluid Mech.* **326**, 417–436.

[14] Morel, P. & Larchevêque, M. 1974 Relative Dispersion of Constant-Level Balloons in the 20mb General Circulation. *J. Atm. Sc.* **31**, 2189.

[15] Nicolleau, F. & ElMaihy, A. 2004 Study of the development of a 3-D material surface and an isoconcentration field using KS. *J. Fluid Mech.* **517**, 229–249.

[16] Nicolleau, F. & ElMaihy, A. 2006 Study of the effect of the Reynolds number on three- and four-particle diffusion in three-dimensional turbulence using Kinematic Simulation. *Phys Rev. E* **74**, 046302

[17] Nicolleau, F. & Vassilicos, J. C. 2000 Turbulent diffusion in stably stratified non-decaying turbulence. *J. Fluid Mech.* **410**, 123–146.

[18] Nicolleau, F. & Vassilicos, J. C. 2003 Turbulent Pair Diffusion. *Phys. Rev. Letters* **90** (2), 024503.

[19] Nicolleau, F. & Yu, G. 2004 Two-particle diffusion and locality assumption. *Phys. Fluids* **16** (4), 2309–2321.

[20] Nicolleau, F., Yu, G. & Vassilicos, J. C. 2007 Kinematic Simulation for stably stratified and rotating turbulence. *Fluid Dyn. Res.* p. In Press.

[21] Obukhov, A. M. 1941 On the distribution of energy in the spectrum of turbulent flow. *Bull. Acad. Sci. U.S.S.R, Géog. & Géophys., Moscow* **5**, 453–466.

[22] Osborne, D. R., Vassilicos, J. C., Sung, K. & Haigh, J. D. 2006 Fundamentals of pair diffusion in kinematic simulations of turbulence *Physical Review E* **74**, 036309.